Analytical Resolution of a Cyclic Two-Way Chromatographic Binary System

C. Castel and M. Sardin
LSGC-CNRS-INPL, F-54001 Nancy, France

M. O. Simonnot
LSGC and EEIGM, F-54000 Nancy, France

The focus is on analytical resolution of the mass-balance relation in the case of a binary ion-exchange system containing chloride and hydrocarbonate anions involved in a two-way chromatographic cyclic process under critical operating conditions, that is, feed and elution solutions with the same total normality and percolation volumes. Local equilibrium theory is used to demonstrate the convergence of the system toward a periodic state and to calculate iteratively the instantaneous and asymptotic concentration profiles inside the separation column. One of the main results is that the calculated chloride composition on the inlet side of the column after the elution step is equal to the chloride composition in the feed solution.

Introduction

The multicomponent equilibrium theory in ion-exchange already has been explained and discussed in detail by many authors (Klein et al., 1967; Tondeur and Klein, 1967; Helfferich, 1967; Helfferich and Klein, 1970; Tondeur, 1969; Rhee et al., 1970, 1971). The principal aim of these articles is the calculation of breakthrough curves and concentration profiles in frontal analysis. Some analytical solutions have been given for ion-exchange systems working under particular operating conditions. But in general there are no analytical solutions for systems containing more than two components.

Analytical results of the equilibrium theory have been used to calculate optimized design specifications for chromatographic cyclic processes in the domain of water softening (Dodds and Tondeur, 1972a,b; 1974). The periodic operating conditions consist of the introduction of feed and elution solutions into the ion-exchange bed at each step of the process. In the softening examples, both solutions are introduced in the same flow direction. The main result is that if the conditions of each step are identifically repeated, a cyclic (periodic) state is reached. In the pressure swing adsorption domain, methods for the direction determination of the periodic state have been proposed (Levan, 1995; Pigorini and Levan, 1997; Dharmashankar Subramanian and Ritter, 1997). A volumetric purge-to-feed ratio parameter is then defined as the purge-gas volume to the feed-gas volume. The theoretical limit for this ratio is unity, below which asymptotic profiles cannot occur inside the column. A new cyclic chromatographic ion-exchange process for the removal of traces of species of weak affinity for ion-exchange resins (Castel, 1998) has been patented (Sardin et al., 1996). The characteristic of this process is that it runs with feed and elution solutions with the same percolation volume and total normality. These conditions characterize the theoretical limit of a generalized elution-to-feed ratio previously defined, which is defined for an ion-exchange system as the number of equivalents brought by the elution solution to the number of equivalents brought by the feed solution. We have shown, numerically and experimentally, that for the selective removal of fluoride ions from natural mineral water, such a system tends to a cyclic steady state, allowing fluoride removal with a satisfactory selectivity (Castel et al., 1999). To optimize the design of cyclic processes, it becomes necessary to characterize the asymptotic concentration profiles as a function of the operating conditions.

In this approach, Levan (1995) assumes the existence of a cyclic steady state and then determines its characteristics. Dharmashankar Subramanian and Ritter (1997) propose an

---

Correspondence concerning this article should be addressed to C. Castel.

analytical solution for the PSA process using equilibrium theory, quantifying the influence of purge-to-feed ratio. What we propose in this article is to pursue this study for constant separation-factor ion-exchange binary systems. Local equilibrium theory in a semi-infinite column is used, and the case of critical purge-to-feed ratio, that is, feed and elution solutions with the same total normality and volume involved in a two-way percolation setup, is analyzed. We will show the instantaneous form and location of the concentration profiles at each point in the feed and elution steps, demonstrate the convergence, and deduce the characteristics of the periodic steady state.

Composition Waves Propagation: Fundamental Relations

Equilibrium theory: Application to a binary ion-exchange system

Fundamental Relation of the Anionic System HCO_3^-/Cl^-. Homovalent anions are involved in an anion-exchange mechanism

$$Cl^- + \overline{HCO_3^-} = \overline{Cl^-} + HCO_3^-, \tag{1}$$

so that the separation factor α can be considered as a constant, defined as follows

$$\alpha = \frac{x_{HCO_3^-} y_{Cl^-}}{y_{HCO_3^-} x_{Cl^-}}. \tag{2}$$

Chloride ions have a higher affinity for the classic anion-exchange resins, which means $\alpha > 1$. Electroneutrality relations in the fluid phase and in the resin phase expressed in ionic fractions give

$$x_{Cl^-} + x_{HCO_3^-} y_{Cl^-} = 1 \tag{3}$$

$$y_{Cl^-} + y_{HCO_3^-} y_{Cl^-} = 1. \tag{4}$$

The complete system admits one variable, x_{Cl^-}, and one parameter, $\alpha > 1$. In the following we pose the developments

$$x = x_{Cl^-} \tag{5}$$

$$y = y_{Cl^-}. \tag{6}$$

To find the solid-phase composition in equilibrium with a given liquid-phase concentration, Eqs. 2, 3, and 4 can be combined to yield

$$y = \frac{\alpha x}{1 + (\alpha - 1)x} \tag{7}$$

which leads to

$$\frac{dy}{dx} = \frac{\alpha}{(1 + (\alpha - 1)x)^2} \tag{8}$$

The assumption of local thermodynamic equilibrium, including the constancy of the volumetric liquid phase flow rate and of the immobile phase void fraction, the isothermality and isochoricity of the exchange, and the absence of dispersion or axial diffusion, give the following relation for the mass balance of the component k

$$\frac{\partial x}{\partial t} + E\frac{\partial y}{\partial t} + v\frac{\partial x}{\partial z} = 0, \tag{9}$$

if $E = [(1-\epsilon)N_e]/\epsilon N_0$, with N_e the exchange capacity, N_0 the total normality, v the pore velocity, and ϵ the porosity. In the present case, Eq. 9 becomes

$$\frac{\partial x}{\partial t} + v_x\frac{\partial x}{\partial z} = 0, \tag{10}$$

with

$$v_x = \frac{v}{1 + E\left(\dfrac{dy}{dx}\right)_x}. \tag{11}$$

According to Eqs. 8 and 11, the propagation velocity of a composition x is as follows

$$v_x = v\frac{[1 + (\alpha - 1)x]^2}{[1 + (\alpha - 1)x]^2 + E\alpha}. \tag{12}$$

Particular Case of Shocks and Compressive Transitions. The foregoing mathematical developments are based on differential mass-balance relations that are only valid for dispersive transitions and continuous distributions of composition. With the assumption of an instantaneous local equilibrium between phases, discontinuities of concentration can exist. The mass-balance relation is in this case replaced by a mass balance around the discontinuity, which gives the following shock velocity (Tondeur, 1987; Tondeur and Bailly, 1987)

$$v_{\Delta x} = \frac{v}{1 + E\left(\dfrac{\Delta y}{\Delta x}\right)_x}. \tag{13}$$

For such a self-sharpening transition, only the boundary values of the transition have a physical meaning

$$v_{\Delta x} = \frac{v}{1 + \dfrac{E\alpha}{[1 + (\alpha - 1)x_F][1 + (\alpha - 1)x_I]}}. \tag{14}$$

Profile calculation during the first two operating cycles

First Saturation Cycle. Let us consider a column (L in length) initially packed with a resin in the hydrogen carbonate form. The straight-flow percolation of a feed solution composed of chloride and hydrogen carbonate ions generates

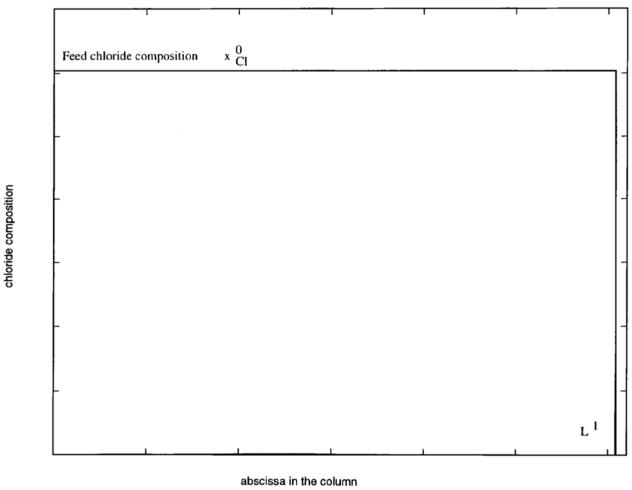

Figure 1. Concentration profile of chloride inside the column at the end of the saturation step.

the propagation of a chloride shock inside the column. The propagation velocity of this shock is

$$v^{\Delta}_{0\to x^0}=\frac{v}{1+\dfrac{E\alpha}{1+(\alpha-1)x^0}}. \tag{15}$$

At the end of the saturation step (duration t_0), the chloride profile inside the column represented in Figure 1 is located at the position:

$$L_1=v^{\Delta}_{0\to x^0}\cdot t_0. \tag{16}$$

First Elution Cycle with Flow Reversal. This step consists of the reverse-flow percolation with the same volume as the feed step of a hydrogen carbonate solution. This step generates an expanding wave of chloride from the bottom to the top of the column because of flow reversal, as described in Figure 2.

The first elution step is not complete. A chloride profile is still present in the column at the end of this step. This final residual profile is well-defined: the abscissa of a composition $x_{HCO_3^-}$ at the end of the elution is

$$z_x=L_1-v_x\cdot t_0 \tag{17}$$

The particular composition $x^{\Delta 1}$ at the inlet of the column is determined as follows:

$$z_{x^{\Delta 1}}=0. \tag{18}$$

Equations 15, 16, and 18 give, for $x=x^{\Delta 1}$

$$x^{\Delta 1}=\frac{\sqrt{(1+(\alpha-1)x^0}-1}{\alpha-1}. \tag{19}$$

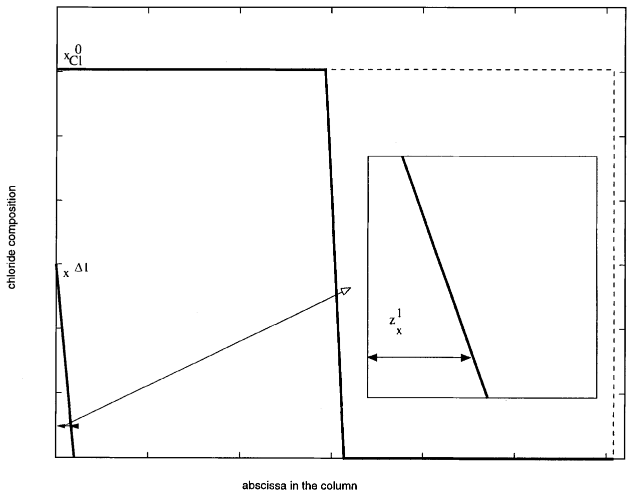

Figure 2. Evolution of the broadening wave of chloride (full line) during the first elution step, with a hydrogen carbonate influent solution of total normality, N_0, and total percolated volume, V_0 (corresponding to t_0).

For $x<x^{\Delta 1}$, the abscissa of a composition x is given by Eq. 17.

Second Saturation Cycle: Combined Wave. The second saturation step is performed with the same operating conditions as the first one. During the feed step, the collision of the shock wave of the feed solution and the compressing wave (residual chloride profile in the column) generates a combined wave, shown in Figure 3, composed of a shock between $x^{\Delta 1}$ and x^0 (higher part) and a compressing wave between 0 and $x^{\Delta 1}$ (lower part).

The initial velocity of the shock is

$$v_{x^{\Delta 1}\to x^0}=\frac{v}{1+\dfrac{E\alpha}{\left[1+(\alpha-1)x^{\Delta 1}\right]\left[1+(\alpha-1)x^0\right]}}. \tag{20}$$

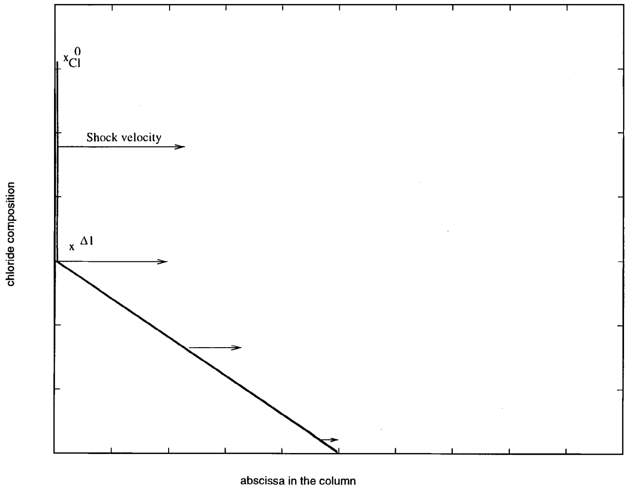

Figure 3. Initial combined concentration profile of chloride at the beginning of the second feed step.

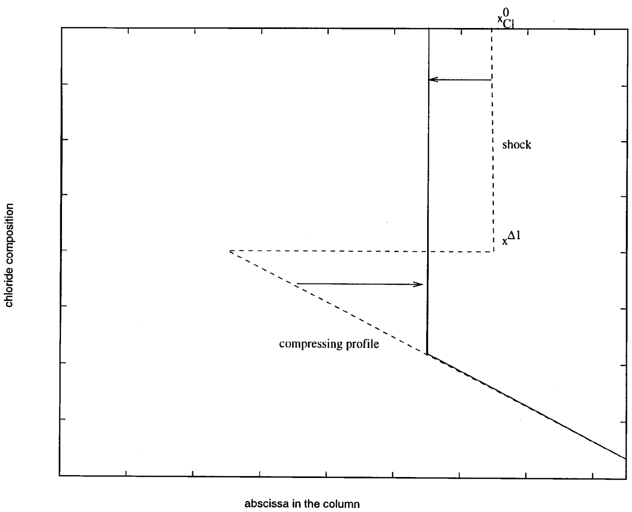

Figure 4. Composition velocity discontinuity (dashed line) of the combined front of chloride and real intermediary front (full line).

Here $x^{\Delta 1}$ also belongs to the compressing front, and its velocity is

$$v_{x^{\Delta 1}} = v \frac{\left(1+(\alpha-1)x^{\Delta 1}\right)^2}{\left(1+(\alpha-1)x^{\Delta 1}\right)^2 + E\alpha}. \tag{21}$$

However, $x^{\Delta 1} < x^0$, therefore $v_{x^{\Delta 1} \to x^0} > v_{x^{\Delta 1}}$.

As shown in Figure 4, $x^{\Delta 1}$ is a point of composition velocity discontinuity. Such a wave (dashed line) cannot exist. An intermediary wave (full line) is developed that fulfills the mass balance around the obtained wave.

The combination of a shock and a compressing wave tends to sharpen the sharpening profile. This means that the shock part of the combined wave reaches the composition $x = 0$ before the total duration of the step, t_0. After the waves cross, the profile becomes a shock again, which travels at the composition velocity:

$$v^{\Delta}_{0 \to x^0_{Cl}} = \frac{v}{1 + \dfrac{E\alpha}{1+(\alpha-1)x^0_{Cl}}} \tag{22}$$

The following development generalizes the results obtained for the first two operating cycles to the subsequent ones.

Generalized Profile Calculation and Determination of the Asymptotic Profile

The fundamental problem is now to determine the nature and the location of the concentration chloride profile at the end of the forward saturation and elution steps. We propose to express L_n and $x^{\Delta n}$ as numerical series of discrete values, which means L_{n+1} is a function of L_n and $x^{\Delta n}$ is a function of L_n.

Remaining chloride concentration profile at the end of the nth elution step

Let us consider q_n as the total remaining quantity of chloride (per unit section of the column) that is still present in both phases of the column after the nth elution step:

$$q_n = \epsilon N_0 \int_0^{x^{\Delta n}} z^n_x \, dx + (1-\epsilon) N_e \int_0^{y^{\Delta n}} z^n_{[x(y)]} \, dy, \tag{23}$$

with

$$y^{\Delta n} = \frac{\alpha x^{\Delta n}}{1+(\alpha-1)x^{\Delta n}} \tag{24}$$

$$x(y) = \frac{y}{\alpha + (1-\alpha)y}. \tag{25}$$

Equation 17 gives

$$z^n_x = L_n - v \frac{[1+(\alpha-1)x]^2}{[1+(\alpha-1)x]^2 + E\alpha} t_0 \tag{26}$$

$$z^n_{[x(y)]} = L_n - v \frac{1}{1 + \dfrac{E}{\alpha}[1+(\alpha-1)y]^2} t_0. \tag{27}$$

Let us pose

$$\chi = 1 + (\alpha-1)x$$

$$\psi = \alpha + (1-\alpha)y.$$

Equation 23 becomes

$$q_n = \epsilon N_0 \left[\int_0^{x^{\Delta n}} L_n \quad dx - t_0 v \int_1^{\chi^{\Delta n}} \frac{\chi^2}{\chi^2 + E\alpha} \frac{d\chi}{\alpha - 1} \right] + \ldots$$

$$+ (1-\epsilon) N_3 \left[\int_0^{y^{\Delta n}} L_n \quad dy - v t_0 \int_\alpha^{\psi^{\Delta n}} \frac{\dfrac{\alpha}{E}}{\dfrac{\alpha}{E} + \psi^2} \frac{d\psi}{1-\alpha} \right], \tag{28}$$

which, after analytic resolution of the integrals, gives

$$q_n = L_n \left[\epsilon N_0 x^{\Delta n} + (1-\epsilon) N_e y^{\Delta n} \right] - \frac{v t_0}{\alpha - 1} \epsilon N_0 \ldots$$

$$\times \left[\chi^{\Delta n} - \sqrt{E\alpha} \arctan \frac{\chi^{\Delta n}}{\sqrt{E\alpha}} - 1 + \sqrt{E\alpha} \arctan \frac{1}{\sqrt{E\alpha}} \right] + \ldots$$

$$- \frac{v t_0}{1-\alpha} (1-\epsilon) N_e \sqrt{\frac{\alpha}{E}} \left[\arctan \frac{\psi^{\Delta n}}{\sqrt{\dfrac{\alpha}{E}}} - \arctan \sqrt{E\alpha} \right]. \tag{29}$$

Determination of the discontinuity composition $x^{\Delta n}$

The elution of the chloride profile with the hydrogen carbonate ion at total normality, N_0, generates a broadening wave of chloride. The new discontinuity point $x^{\Delta n}$ (composition of the solution at the top of the column) is given by the solution of Eq. 18:

$$L_n = v\frac{[1+(\alpha-1)x]^2}{[1+(\alpha-1)x]^2+E\alpha}t_0 \tag{30}$$

$$x^{\Delta n} = \frac{\sqrt{\dfrac{\dfrac{L_n E\alpha}{vt_0}}{1-\dfrac{L_n}{vt_0}}}-1}{\alpha-1}. \tag{31}$$

Iterative calculation of L_n

We have previously seen that the concentration profiles at the end of the saturation steps were shocks because of the acceleration due to combined waves. For the location of the shock corresponding to the cycle $n+1$, the global mass balance gives:

$$L_{n+1} = \frac{q_0+q_n}{\epsilon N_0 x^0 + (1-\epsilon)N_e y^0} \qquad \text{for} \qquad n \geq 1 \tag{32}$$

$$L_1 = \frac{vt_0}{1+\dfrac{E\alpha}{1+(\alpha-1)x^0}}, \tag{33}$$

with

$$q_0 = N_0 x^0 \epsilon v t_0 \tag{34}$$

the quantity injected per cycle in the column expressed in number of equivalent per section area.

Equations 29, 31, and 32 allow us to express L_{n+1} as a discrete function of L_n.

Convergence of the numerical series of elements $x^{\Delta n}$ *and* L_n

Evolution of $x^{\Delta n}$ *and* L_n.

- The combined wave makes the compressing front sharpen faster so that the shock reaches the composition $x = 0$ before t_0. Then it can be concluded that

$$L_n > L_{n+1}. \tag{35}$$

- $x^{\Delta n}$ is the solution given by Eq. 31. The function

$$v\frac{[\alpha+(1-\alpha)x]^2}{[\alpha+(1-\alpha)x]^2+E\alpha}t_0$$

is an increasing function of the parameter x. Relation 35 gives

$$x^{\Delta n} > x^{\Delta n-1}. \tag{36}$$

Because the total normality is constant for both feed and elution solution, there is no normality interference and $x^{\Delta n}$ has an upper limit of x^0. This series of discrete values then admits a limit $x^{\Delta n \text{limit}}$ when n tends to infinity and $x^{\Delta n \text{limit}} \leq x^0$. After the saturation and elution steps, the concentration profile admits an asymptotic limit profile expressed as L_{limit} for the shock at the end of the saturation step.

Asymptotic Profile. We have previously shown that the discrete function $x^{\Delta n}$ tended to a limit, $x^{\Delta n \text{limit}}$, that is inferior or equal to x^0. If this limit is strictly inferior to x^0, it still remains a composition velocity discontinuity that, because of the combined wave, generates an increase in L_n, and consequently an increase in $x^{\Delta n}$ for the next cycle. If $x^{\Delta n \text{limit}}$ is inferior to x^0, the system cannot be at the steady state, so $x^{\Delta n \text{limit}}$ is equal to x^0. The corresponding value of the saturation profile is then given by Eq. 12, expressed in chloride composition:

$$L_{\text{limit}} = v\frac{[1+(\alpha-1)x^0]^2}{[1+(\alpha-1)x^0]^2+E\alpha}t_0. \tag{37}$$

Numerical Application

The iterative calculation of these parameters for the first thousand complete cycles is plotted in Figures 5 and 6 for the operating conditions presented in Table 1. The abscissa and discontinuity point corresponding to the thousandth cycle are

$$L_{1,000} = 0.31485 \text{ m}$$

$$x^{\Delta 1,000} = 0.030138.$$

These results are in agreement with the theoretical values of the asymptotic limits:

$$L_{\text{limit}} = 0.31490 \text{ m}$$

$$x^{\Delta n \text{limit}} = x^0 = 0.0302.$$

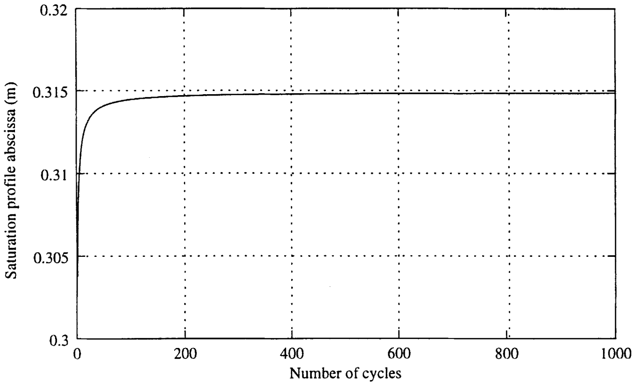

Figure 5. Location of the concentration profile at the end of the saturation step for the operating conditions presented in Table 1.

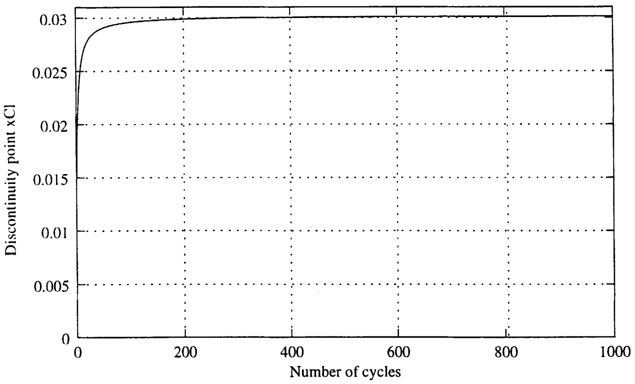

Figure 6. Discontinuity concentration $x^{\Delta n}$ at the end of the elution step for the operating conditions presented in Table 1.

Discussion

A *binary heterovalent system*, for example, SO_4^{2-}/HCO_3^-)

$$SO_4^{2-} + 2\overline{HCO_3^-} = \overline{SO_4^{2-}} + 2HCO_3^-, \tag{38}$$

with

$$\alpha_{HCO_3^-}^{SO_4^{2-}} = \alpha = \frac{y_{SO_4^{2-}}(x_{HCO_3^-})^2}{x_{SO_4^{2-}}(y_{HCO_3^-})^2}, \tag{39}$$

behaves quantitatively in the same manner as a homovalent one. The results concerning the convergence of the concentration profiles can be directly applied. A new analytical difficulty arising here is the resolution of a second-degree equation for the equilibrium isotherm

$$y_{SO_4^{2-}} = 1 + \frac{\alpha\left(1 - x_{SO_4^{2-}}^2\right) - \left(1 - x_{SO_4^{2-}}\right)\sqrt{\alpha^2\left(1 - x_{SO_4^{2-}}^2\right) + 4\alpha x_{SO_4^{2-}}}}{2x_{SO_4^{2-}}}, \tag{40}$$

and hence of the velocities given by Eqs. 11 and 13. An approximate solution could be easily calculated that considers the heterovalent system as a homovalent one $\text{Sulfate}^-/HCO_3^-$ and keeping $y_{SO_4^{2-}} = y_{\text{Sulfate}^-}$. The new constant separation factor would then be

$$\alpha_{HCO_3^-}^{\text{Sulfate}^-} = \frac{y_{\text{Sulfate}} - x_{HCO_3^-}}{x_{\text{Sulfate}} - y_{HCO_3^-}}, \tag{41}$$

derived from Eq. 39.

Theoretical asymptotic profiles can be characterized by deriving the expression of the isotherm (Eq. 40):

$$\frac{dy_{SO_4^{2-}}}{dx_{SO_4^{2-}}}\left(x_{SO_4^{2-}}^0\right) = \frac{-2\alpha\left(1 - x_{SO_4^{2-}}^0\right)\left(1 + x_{SO_4^{2-}}^0\right)}{4\left(x_{SO_4^{2-}}^0\right)^2} + \dots$$
$$+ \frac{\left[\left(x_{SO_4^{2-}}^0\right)^2 - x_{SO_4^{2-}}^0 + 2\right]\sqrt{\alpha^2\left(1 - x_{SO_4^{2-}}^0\right)^2 + 4\alpha x_{SO_4^{2-}}^0}}{4\left(x_{SO_4^{2-}}^0\right)^2} \tag{42}$$

$$x_{SO_4^{2-}}^{\Delta n\,\text{limit}} = x_{SO_4^{2-}}^0$$

$$z_{\text{sat}}^{\text{limit}} = \frac{\upsilon t_0}{1 + E\left(\dfrac{dy_{SO_4^{2-}}}{dx_{SO_4^{2-}}}\right)_{x^0 SO_4^{2-}}}.$$

The *number of operating cycles* required to reach the periodic steady state is an important parameter for the control of an experimental setup. The calculated limits for both have not yet been reached by the thousandth cycle, which leads to the conclusion that the steady state has not yet been reached. But the relative errors in $L_n(m)$ and $x^{\Delta n}$ between the 999th and the 1,000th cycles are less than 0.000014 and 0.0002%, respectively, and between the theoretical limits and the values of $L_n(m)$ and $x^{\Delta n}$ are, for the 50th cycle, already less than 0.26 and 3.70%, respectively. Differences in this magnitude are experimentally rapidly undetectable because of analytical inaccuracies and volumetrically averaged compositions. Previous experiments (Castel et al., 1999) have demonstrated that effluent compositions are stable after the twentieth cycle.

Conclusion

Starting from the first operating cycles and calculating iteratively the characterizations (L_{limit} and $x^{\Delta n\text{limit}}$) of the final concentration profiles, we have demonstrated the convergence of a HCO_3^-/CL^- system under cyclic operating conditions with flow reversal and for a purge-to-feed ratio equal to 1 toward a periodic steady state. The asymptotic profiles corresponding to this steady state can be calculated *a priori* from the data of the system. The calculated limit chloride composition at the top of the column at the end of the elution step $x^{\Delta n\text{limit}}$ gives $x^{\Delta n\text{limit}}$, which is equal to x^0, in agreement with the results of Levan (1995) concerning the PSA process, which works with a volumetric purge-to-feed ratio equal to unity. If necessary, the composition exhibits strong analogies of reasoning in the large domain of preparative chromatography. This article focuses on the problem of available energy. A direct application of these developments is the patented ion-exchange process for selectively removing fluoride ions

Table 1. Operating Conditions of the First Thousand Iterative Calculation of L_n and $x^{\Delta n}$

α	2.2
x_{Cl}^0	0.0302
υ	2.78bx10^{-3}m/s
ϵ	0.5
N_e	2 eq/L
N_0	3.28×10^{-2} eq/L
t_0	14,400 s

(Sardin et al., 1996), which works under the critical purge-to-feed ratio. For ion-exchange processes, the energy is indeed introduced by the elution solution in terms of number of equivalents. We have experimentally shown (Castel et al., 1999) that such a critical system can converge toward an applicable cyclic steady state, if the experimental conditions of volume and hydrodynamics are fulfilled, that is, with percolated volumes greater than the porous volume, with column packings that do not have significant dead volumes or short circuits, and with solutions whose densities allow good mixing.

Notation

$\bar{A}$ = species A adsorbed on the solid
L_n = longitudinal position of the shock at the end of the nth feed step, m
L_{limit} = longitudinal abscissa of the asymptotic profile at the end of the feed step, m
N_0 = total normality of a solution, eq/L
N_e = total exchange capacity of the ion-exchange resin, eq/L
q_0 = quantity of chloride injected per cycle in the system, eq/m^2
q_n = total remaining quantity of chloride in the column at the end of the elution step of the cycle n
t = time, s
t_0 = duration of an operating cycle, s
v = interstitial velocity of the fluid, m/s
v_x = composition velocity of the ionic fraction x, m/s
$v^{\Delta}_{x_1 \to x_2}$ = composition velocity of a shock between x_1 and x_2
x = ionic fraction in the liquid phase
x^0_{Cl} = ionic fraction of the chloride in the feed solution
$x^{\Delta n}$ = ionic fraction of the discontinuity point at the end of the elution step in the liquid phase of the column
$x^{\Delta \text{limit}}$ = ionic fraction of the discontinuity point at the steady state
y = ionic fraction in the solid phase
$y^{\Delta n}$ = ionic fraction of the discontinuity point at the end of the elution step in the solid phase of the column
z = longitudinal abscissa, m
z^n_x = longitudinal position of the composition x at the end of the nth elution step, m

α = separation factor
ϵ = porosity factor
χ = variable function of α and x
ψ = variable function of α and y

Literature Cited

Castel, C., "Elimination d'Especes Traces en Solution. Conception et Developpment d'Un Procede d'Echange d'Ions Selectif Cyclique," PhD Diss., Institut National Polytechnique de Lorraine (INPL), Nancy, France (1998).

Castel, C., M. O. Simonnot, and M. Sardin, "Selective Removal of Fluoride Ions by a Two-Way Ion-Exchange Cyclic Process," *Chem. Eng. Sci.*, **55**, 3341 (2000).

Dharmashankar S., and J. A. Ritter, "Equilibrium Theory for Solvent Vapor Recovery by Pressure Swing Adsorption: Analytical Solution for Process Performance," *Chem. Eng. Sci.*, **52**(18), 3147 (1997).

Dodds, J. A., and D. Tondeur, "The Design of Cyclic Bed in Ion-Exchange Operation. I A Predictive Method Applied to a Simple Softening Cycle," *Chem. Eng. Sci.*, **27**, 1267 (1972a).

Dodds, J. A., and D. Tondeur, "The Design of Cyclic Bed in Ion-Exchange Operation. II The Effects of Changes in Total Concentration," *Chem. Eng. Sci.*, **27**, 2291 (1972b).

Dodds, J. A., and D. Tondeur, "The Design of Cyclic Bed in Ion-Exchange Operation. III Softening Solutions Containing Na^+, Mg^{2+}, Ca^{2+}," *Chem. Eng. Sci.*, **29**, 611 (1974).

Helfferich, F. G., "Multicomponent Ion-Exchange in Fixed Beds. Generalized Equilibrium Theory for Systems with Constant Separation Factors," *Ind. Eng. Chem. Fundam.*, **6**, 362 (1967).

Helfferich, F. G., and G. Klein, *Multicomponent Chromatography*, Dekker, New York (1970).

Klein, G., D. Tondeur, and T. Vermeulen, "Multicomponent Ion Exchange in Fixed Beds. I. General Properties of Equilibrium Systems," *Ind. Eng. Chem. Fundam.*, **6**, 339 (1967).

Levan, M. D., "Pressure Swing Adsorption: Equilibrium Theory for Purification and Enrichment," *Ind. Eng. Chem. Res.*, **34**, 2655 (1995).

Pigorini, G., and M. D. Levan, "Equilibrium Theory for Pressure Swing Adsorption. 3. Separation and Purification in Two Component Adsorption," *Ind. Eng. Chem. Res.*, **36**, 2306 (1997).

Rhee, H. K., R. Aris, and N. R. Amundson, "On the Theory of Multicomponent Chromatography," *Phil. Trans. R. Soc. London*, **267**, 419 (1970).

Rhee, H. K., R. Aris, and N. R. Amundson, "Multicomponent Adsorption in Continuous Countercurrent Exchangers," *Phil. Trans. R. Soc. London*, **269**, 187 (1971).

Sardin, M., M. O. Simonnot, and C. Castel, "Procede Pour Reduire Selectivement la Concentration de l'Une des Especes Presente en Solution," French Patent No. 272 68 19 (1996).

Tondeur, D., "Theorie des Colonnes Echangeuses d'Ions," PhD Diss., INPL, Nancy, France (1969).

Tondeur, D., and G. Klein, "Multicomponent Ion-Exchange in Fixed Beds. Constant Separation Factor Equilibrium," *Ind. Eng. Chem. Fundam.*, **6**, 351 (1967).

Tondeur, D., "Unifying Concept in Nonlinear Unsteady Processes. Part I: Solitary Travelling Waves," *Chem. Eng. Processes*, **21**, 167 (1987).

Tondeur, D., and M. Bailly, "Unifying Concept in Nonlinear Unsteady Processes. II. Multicomponent Waves, Competition and Diffusion," *Chem. Eng. Processes*, **22**, 91 (1987).

Manuscript received June 15, 2000, and revision received Aug. 1, 2001.